

Photoinduced charge transfer from quantum dots measured by cyclic voltammetry

Micaela K. Homer^a, Ding-Yuan Kuo^a, Florence Y. Dou^a and Brandi M. Cossairt^{a*}

^aDepartment of Chemistry, University of Washington, Box 351700, Seattle, WA 98195-1700.

*Email: cossairt@uw.edu

Abstract

Measuring and modulating charge-transfer processes at quantum dot interfaces are crucial steps in developing quantum dots as photocatalysts. In this work, cyclic voltammetry under illumination is demonstrated to measure the rate of photoinduced charge transfer from CdS quantum dots by directly probing the changing oxidation states of a library of molecular charge acceptors, including both hole and electron acceptors. The voltammetry data demonstrates the presence of long-lived charge donor states generated by native photodoping of the quantum dots as well as a positive correlation between driving force and rate of charge transfer. Changes to the voltammograms under illumination follow mechanistic predictions from classic zone diagrams and electrochemical modeling allows for measurement of the rate of productive electron transfer. Observed rates for photoinduced charge transfer on the order of 0.1 s^{-1} are calculated, which are distinct from the picosecond dynamics measured by conventional transient optical spectroscopy methods and are more closely connected to the quantum yield of light mediated chemical transformations.

Introduction

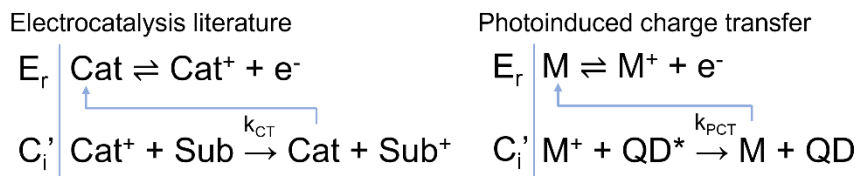
Photoinduced charge separation is a key step in artificial photosynthesis for the conversion of solar energy to high-value chemical compounds.¹ Quantum dots (QDs) have long been promoted as ideal photosensitizers for photocatalysis due to their high extinction coefficients, electronic tunability, and solution processability,² but efficient extraction of high energy charge carriers from QDs remains a design challenge.³ Photoinduced charge transfer from QD donors requires transfer of charges across a complex interface between the inorganic QD core and a molecular cocatalyst or substrate in solution.^{4,5} This complicated interface comprises a high prevalence of defect electronic states in the QD,^{6,7} and the covalent and non-covalent interactions between the QD, the insulating ligand shell, and the charge acceptor.⁸ Conventional models of charge transfer in molecular systems (e.g. the two state system described by the Marcus formalism) are therefore insufficient to predict the rate of useful charge extraction from QDs, prompting experimental exploration.⁹

Photoluminescence spectroscopy¹⁰⁻¹² and transient absorbance spectroscopy^{13,14} are frequently employed to determine rates of photoinduced charge transfer in QD systems. In these experiments, the charge transfer process measured is pseudo-unimolecular with a first-order rate constant. This rate presumes pre-adsorption of the charge acceptor to the QD and does not consider freely diffusing charge acceptors nor the dynamic noncovalent chemical interactions between the QD and acceptor.^{10,13,15,16} While determination of the first order rate has utility, especially when compared with other unimolecular photophysical processes such as electron/hole recombination, there is a large disconnect in the literature between the time scale for this fundamental process (picoseconds) and the time scale of photocatalytic

reactions (minutes)^{17,18}. It may then be counterintuitive that several reports have found that the rate-limiting step of photocatalysis is charge transfer from nanocrystal photosensitizers to substrate or cocatalyst.¹⁸⁻²¹ This disconnect begs us to consider that the spectroscopic first order rate of charge transfer does not accurately report on the rate of production of charge separated states, and instead a new method is needed to understand processes taking place on the same time scales as chemical reactions.³

Alternatively, charge transfer can be rationalized as a bimolecular reaction that is first order with respect to both the charge donor (excited QD) and acceptor (substrate).²² The two species must first collide before charge can be extracted from the QD, and the rate of observed charge extraction will depend on the frequency of collisions, the rate of the fundamental photophysical process observed by time-resolved spectroscopies, and the fraction of collisions that allow strong electronic coupling between the QD and charge acceptor.

To this end, we turned to cyclic voltammetry (CV), a measurement tool that directly probes the changing oxidation state of a redox active small molecule. CV has been employed in homogeneous electrocatalysis literature as a probe for the changing oxidation states of a molecular electrocatalyst,²³ and has been theorized to be a tool for evaluating molecular photoelectrocatalysis.²⁴ We hypothesized that CV could be extended to systems involving photoinduced charge transfer from QDs. In the electrocatalysis literature, one of the simplest and most well-understood systems is described by two reactions: the oxidation and reduction of the electrocatalyst at the electrode, and the catalytic reaction in which the electrocatalyst transfers charge to substrate. This mechanism is termed E_rC_i' . In such a system, the CV is modulated as compared to CVs in the absence of substrate, and this modulation can be quantified to obtain the rate constant for the catalytic reaction. For a thorough review of this technique, see Rountree *et al.*²³ In this work we aim to analogously measure the rate of productive charge extraction from QDs using CV (**Scheme 1**). We believe that the rates obtained through this measurement (k_{PCT}) will accurately reflect the extraction of charge from QDs and will bridge the gap in time scales between photophysics and chemical transformations.



Scheme 1. The E_rC_i' mechanism employed in the electrocatalysis literature (left), and the extension of this mechanism to photoinduced charge transfer from an excited QD (QD*) to a molecular acceptor (M). In this work, k_{PCT} represents the intrinsic rate constant of photoinduced charge transfer.

Materials and Methods

Photoelectrochemistry cell design

A traditional three-electrode electrochemical cell was modified for *in situ* illumination. A 448 nm LED (Luxeon Star, equipped with a 12° beam optic, FWHM 20nm) was positioned under a quartz cuvette with a polished bottom and open top (**Figure 1**). The cuvette was placed on top of the LED. The LED was powered by a DC power supply (Nice-Power). The driving current was 0.2-0.8A, corresponding to approximately 0.3-1.1W of illumination.

Holes were drilled in a cuvette cap for the three electrodes and the glassy carbon disc working electrode (BASi) was epoxied to the cap, ensuring the light had a constant and known pathlength (0.67 mm) through the solution to the active area of the working electrode. The pathlength is small to minimize undesired convection effects on the voltammogram from photoirradiation,²⁵ as well as to decrease the amount of light that is attenuated by the highly absorbent QDs in solution before reaching species near the working electrode surface. The counter electrode was a platinum wire, and the pseudo-reference electrode was a silver wire in a ceramic-fritted glass tube (Pine) filled with 0.1M [TBA][B(C₆F₅)₄].

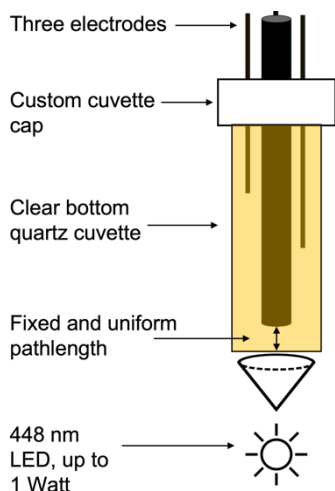


Figure 1. Drawing of the electrochemical cell for voltammetry under illumination.

Solvent and electrolyte design for photoelectrochemistry

The selection of solvent and supporting electrolyte is critical to obtaining electrochemical measurements suitable for quantitatively monitoring photoinduced charge transfer. The solvent reorganizes to facilitate charge transfer, both from the working electrode to the redox probe and between the QD and the redox probe, so it must be polar to minimize internal resistance. The solvent must also allow high electrolyte concentration and have a wide electrochemical window to screen a wide range of redox probes. These electrochemical considerations are general, but for photoelectrochemistry, the solvent must additionally not undergo any photodecomposition nor reactivity with excited QDs. Previously, our group has found that a mixture of 9:1 THF:MeCN was able to suspend oleic acid capped QDs with low internal resistance.²⁶ However, when THF was used in this work, the CV exhibited current crossover (**Figure S1**), an unusual observation that indicates that the product of Faradaic oxidation on the forward scan of the CV has been chemically converted to another species that is more easily oxidized and observed on the backward segment.²⁷ Given prior observations that THF degrades under illumination to form reactive radicals,²⁸ THF is not a suitable solvent for this study.

Dichloromethane was another attractive solvent due to its modest polarity and ability to disperse as-synthesized QDs. Unfortunately, CVs under illumination displayed oscillations in the current, especially in the diffusion limited regime (**Figure S2**). These oscillations were the result of gas bubbles evolving and reaching the surface of the working electrode, which was observed visually during illumination of the sample. Headspace analysis detected production of methane after illumination (**Figure S3**). With these observations, as well as prior observation of dehalogenation of CH₂Cl₂ with QD photocatalysts²⁹, we

conclude that the system photocatalytically dehalogenates CH_2Cl_2 to methane, so CH_2Cl_2 is not a suitable choice for photoelectrochemical measurement.

Another limitation in solvent choice is the solubility of the QDs, as QDs are often natively capped with aliphatic ligands that prevent dispersion in polar solvent at high electrolyte concentration. Ligand exchange was performed on QDs to replace the native oleic acid ligand shell with 2-[2-(2-Methoxyethoxy)ethoxy]acetic acid (MEEAA), which is known to be an amphiphilic ligand that has dissolved nanocrystals in solvents ranging from toluene to water.^{30,31} In our hands, 3.8 nm CdS QDs capped with this ligand are readily soluble in a variety of polar solvents, including water, acetone, and ethanol, but cannot be dispersed in some polar, aprotic solvents suitable for electrochemistry such as acetonitrile and propylene carbonate. Ultimately, benzonitrile (PhCN) was selected for this study because of the good colloidal stability of QDs in electrolyte solutions prepared using this solvent. MEEAA capped QDs in benzonitrile solution remain suspended for at least several months even in the presence of electrolyte.

Finally, the solvent and electrolyte should allow reversible CVs for all the redox probes in the absence of QDs and illumination. Using the more common tetrabutylammonium salt of the $[\text{PF}_6]^-$ anion prevented reversible redox behavior of ferrocenecarboxylic acid (FcCOOH), presumably due to the high electrophilicity of the $[\text{FcCOOH}]^+$ cation. Instead, the tetrabutylammonium salt of the weakly coordinating anion $[\text{B}(\text{C}_6\text{F}_5)_4]^-$ was used. This completely fluorinated phenyl borate is known to stabilize organometallic cations, such that the only allowed processes in the CVs were oxidation and reduction of the metal center.³² When this anion was used in the supporting electrolyte, FcCOOH displayed nearly ideal electrochemical reversibility.³³

Results and Discussion

Photodoping and slow electron trapping observed by CV

By illuminating the sample, the chemical reaction in the $\text{E}_r\text{C}_i'$ mechanism is turned on, and we observe distortion of the CV shape. Classically, the shape of the CV in this mechanism can be described by a zone diagram (**Figure 2a**), where the zone observed will depend on the concentrations of charge donor and acceptor, as well as the scan rate and the intrinsic rate of charge transfer. Generally, the solution in the electrochemical cell was 1.1×10^{-5} M QDs and approximately 130 equivalents of the redox probe. After beginning illumination of a solution of CdS QDs with ferrocene a representative redox probe, successive CV scans continue to distort as compared to the dark trace for several minutes (**Figure 2b**). The CVs move to the right across the $\text{E}_r\text{C}_i'$ zone diagram, from zone D to zone KD to zone KS, which by analogy to electrocatalysis literature²³ demonstrates an increase in the concentration of charge donor states (herein represented as $[\text{QD}^*]$) (**Figure 2a,b**). This distortion occurs over ca. 20 minutes of illumination and then stabilizes, corresponding to a stabilization of $[\text{QD}^*]$. This extremely long time scale until equilibration of $[\text{QD}^*]$ as compared to the speed of photoexcitation (femtoseconds) suggests that the charge donor state is not simply an exciton, but rather the product of a slow chemical process following excitation. Some excitons may directly act as charge donors, but exciton dissociation directly to the molecular probe is not the only process observed.

Previous studies have reported native n-type photodoping in cadmium chalcogenide QDs over the same timescale observed in this study, wherein after excitation a valence band hole is extracted without any added reductant, leaving behind a long-lived conduction band electron.^{34,35} To further investigate the

nature of the charge donor state, we monitored the solution with successive CV scans after illumination was stopped. Over the course of ca. 20 minutes, the CV recovers back to its original dark trace as QD^* is slowly depleted to zero, thus tracking to the left along the E_rC_i' zone diagram (**Figure 2c**). Others have also reported that negatively photodoped QDs live for many minutes due to extremely slow conduction band electron trapping.^{34–36} The long-lived electron donor state herein may be long-lived conduction band electrons and/or electrons trapped as reduced surface Cd,^{37–40} but this technique alone cannot deconvolute the two. While this work deals with QDs that natively photodope, the technique is agnostic to the specific nature of the electron donor state. The changing oxidation state of the redox probe is being measured rather than changing photophysics of the QD, so the measurement is general regardless of the identity of the charge donor state.

While $[QD^*]$ stabilizes for a given light intensity after many minutes, the stable CVs of a representative redox probe, $FcCOOH$ are not the same when the light intensity is varied. As the power of illumination is increased from 0.33 W to 1.14 W, the stable CV is distorted further from the dark CV, again well matched to traversing to the right across the zone diagram (**Figure 2d**). This observation indicates that although at any given light intensity $[QD^*]$ reaches an equilibrium, a maximum concentration of charge donors has not been reached. It is expected that as light intensity is further increased, the CV would eventually stop distorting, but this light-saturated regime is not observed due to the limited power output of the LED light source.

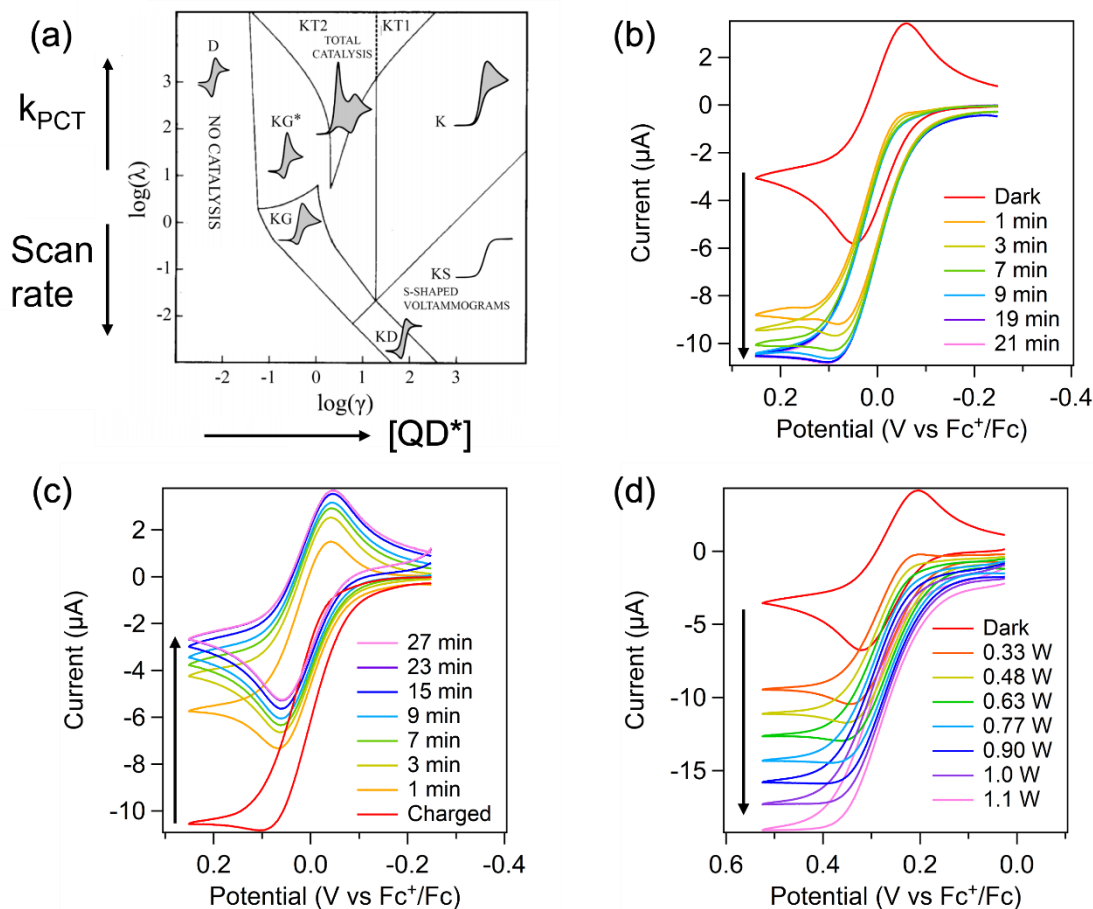


Figure 2. (a) The zone diagram for the E_rC_i' mechanism, adapted from Rountree et al *Inorg. Chem.* 2014, 53, 19, 9983–10002 Copyright 2014 American Chemical Society (b) Increase in $[QD^*]$ monitored by

successive CV scans of Fc after illumination begins. (c) Depletion of charge donor states by slow electron trapping monitored by CVs of Fc after illumination ends. (d) Light intensity dependence on equilibrated CVs of FcCOOH. 0.1M [TBA][B(C₆F₅)₄], benzonitrile, glassy carbon working, Pt counter, Ag wire pseudo reference electrodes, 10 mV/s.

Electron acceptors: Co(Cp)(dppe), FcNH₂, Fc, FcCOOH, FcCOCH₃

When QDs are added to solutions of Co(Cp)(dppe) (Cp = cyclopentadienyl, dppe = 1,2-Bis(diphenylphosphino)ethane), aminoferrocene (FcNH₂), ferrocene (Fc), FcCOOH, or acetylferrocene (FcCOCH₃) the CV remains unchanged for traces without illumination. This observation, alongside no observed change in the dark open circuit potential, demonstrates that none of these probes exhibit charge transfer reactions with the QDs in the dark. Furthermore, the magnitude of the current does not change upon addition of QDs to the probes in the dark, indicating no adsorption to the QDs. If indeed there was adsorption, the effective diffusion coefficient of the redox probes would decrease due to the much larger QD, decreasing the current measured in CV. Previously, FcCOOH was observed to bind to oleate-capped CdSe QDs using CV through carboxylate-carboxylate exchange with the native ligand shell.²⁶ In contrast, FcCOOH does not undergo similar exchange with MEEAA-capped CdS QDs. The lack of exchange is rationalized by the lower pK_a of MEEAA (pK_a = 3.61)⁴¹ compared to oleic acid (pK_a = 9.85)⁴².

The CVs of solutions containing Co(Cp)(dppe), FcNH₂, Fc, FcCOOH, and FcCOCH₃ and QDs all distort under illumination, and stabilize after several minutes as described in the photodoping discussion above. For all probes at all light intensities and scan rates, there is an increase in oxidative current and decrease of reductive current as compared to dark traces (**Figure 3a**). This implies that under illumination, the oxidized probe, M⁺, is reduced to M through photoinduced electron transfer from the quantum dot. To elaborate, during the oxidative segment of the CV, as the potential is increased, M is oxidized to M⁺ at the working electrode (E_r in **Scheme 1**). Then, some of this M⁺ is reduced back to M by QD* (C_i in **Scheme 1**). This additional M can be oxidized at the electrode and so on, increasing the measured oxidative current as compared to the dark scan. On the reductive segment, M⁺ formed at the electrode has been depleted by photoinduced charge transfer, so the magnitude of the reductive current is decreased. At steady state, the rate of M⁺ depletion is equal to M⁺ generation at the working electrode. [M⁺] is zero at the electrode surface, so there is no reductive current.

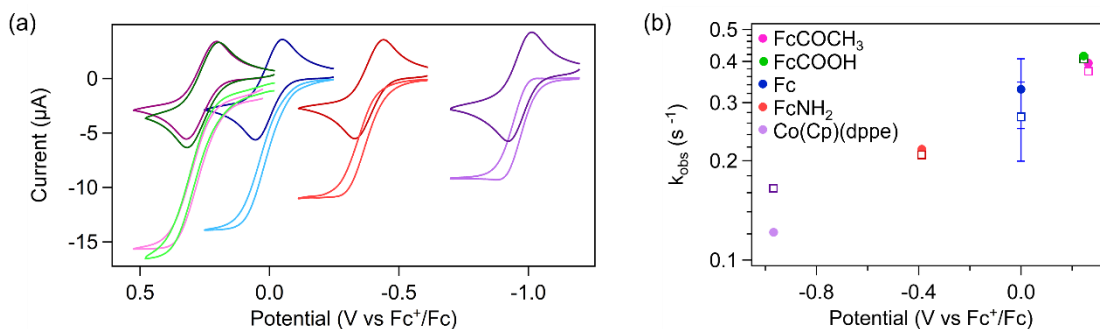


Figure 3. (a) CVs of the series of electron acceptors without illumination (dark colors) and with 1.1 W illumination (light colors). From left to right, the redox probes are FcCOCH₃ (fuchsia), FcCOOH (green), Fc (blue), FcNH₂ (red), and Co(Cp)(dppe) (purple). (b) The rate constant for photoinduced charge transfer under 0.77 W illumination determined mathematically (open squares) and by electrochemical modeling

assuming a large value of γ (closed circles), plotted against the redox potential of each probe. Error bars on the Fc data point were obtained from quadruplicate experiments.

Mathematical Determination of $E_r C_i'$ Rate Constant for Co(Cp)(dppe), FcNH₂, Fc, FcCOOH, FcCOCH₃

The rate constant for the photoinduced charge transfer reaction (C_i' in the $E_r C_i'$ mechanism) can be determined mathematically from voltammograms when in zone KD or KS, which are the zones observed in this work. In these experiments, the observed rate in the experiment (k_{obs}) is related to the scan-rate independent plateau current (i_c) observed in zone KS and zone KD by Equation 1, where n is the number of electrons transferred at the electrode, and i_p and v are the peak current and scan rate for a reversible, dark experiment. Notably, this equation does not require any knowledge of the diffusion coefficient or concentration of the redox probe because the currents are taken as a ratio.

$$\frac{i_c}{i_p} = \frac{1}{0.446} \sqrt{\frac{RT}{nFv}} k_{obs} \quad (\text{Eq. 1})$$

A plot of i_c/i_p against the inverse square root of scan rate for several dark scans yielded a straight line with a slope related to k_{obs} and constants only (**Figure S4**). The forward rate, k_{obs} , is a direct reporter on the rate of effective charge extraction and is distinct from values obtained spectroscopically. k_{obs} is plotted against the redox potential of the charge-accepting probes in **Figure 3b**. For a plot against the estimated driving force for electron transfer, see **SI Figure S5**.

Uncertainty in [QD*] results in uncertain intrinsic rate

The intrinsic rate constant, k_{PCT} , is related to k_{obs} by Equation 2.

$$k_{obs} = k_{PCT}[QD^*] \quad (\text{Eq. 2})$$

It is experimentally challenging to determine the concentration of charge donors in the system, [QD*], especially given that these charge donors may be electrons from excitons, conduction band electrons in photodoped QDs, or reduced surface traps. The simplest starting hypothesis is that [QD*] is approximately equal to the analytical concentration of QDs, [QD]₀. In this assumption, each QD has one conduction band electron that is available for charge transfer. Others have shown that while multi-excitation is possible,⁴³ the maximum average number of excess conduction band electrons is about one per QD.^{34,36,44,45} If we estimate that each QD has exactly one conduction band electron ready for electron transfer, then [QD*] = [QD]₀ = 1.1 × 10⁻⁵ M and k_{PCT} is on the order of 10⁴ M⁻¹s⁻¹.

Though estimating [QD*] = [QD]₀ has solid conceptual backing, this value cannot explain the data with a simple $E_r C_i'$ mechanism. The CVs taken during illumination pass from zone D to KD to KS (**Figure 2a, b**). In electrocatalysis literature, zones KS and KD are observed when operating under conditions of no substrate consumption due to large excess of substrate compared to the concentration of catalyst. By analogy, this implies that zones KS and KD should only be observed when QD* is not consumed by the charge transfer reaction. This could occur when either QD* is in excess compared to the molecular probe M or when QD* is regenerated once an electron is transferred from QD* to M⁺, effectively making [QD*] constant despite being small. The amount QD* is in excess compared to M is quantified by the

dimensionless parameter γ , defined in Equation 3. With only the two reactions in the E_rC_i' mechanism, zone KS should only be observed when $\log(\gamma) > 1$.

$$\gamma = \frac{[QD^*]}{[M]} \quad (\text{Eq. 3})$$

If $[QD^*] = [QD]_0$, then $\log(\gamma) \approx -2$ and M is in excess, not QD^* . So, if we assume $[QD^*] = [QD]_0$ then QD^* must be regenerated to explain the experimental data. This conclusion is exemplified by electrochemical modeling of CVs in DigiElch. When $[QD^*] = [QD]_0$ without an explicit regeneration step, the modeled CVs show very little deviation from the ground state dark CVs, regardless of the rate of charge transfer, because there is so little QD^* compared to the redox probe and it is quickly depleted at the electrode (**Figure S6**). When a third reaction for the fast regeneration of QD^* was added to the model, we can model the data even with small values of γ (**Figure 4**, modeling details in SI). The modeled values of k_{PCT} when fast regeneration is added to the model are on the order of $10^4 \text{ M}^{-1}\text{s}^{-1}$, and inputting $[QD^*] = [QD]_0$ into Equation 2 gives observed rates on the order of 0.1 s^{-1} (**Figure S7**).

During illuminated studies, regeneration of QD^* makes good sense; after electron transfer the QD can be re-excited. However, when illumination is stopped, there cannot be any photoinduced regeneration of QD^* at the electrode, but the CVs are still in zone KD (**Figure 2c**). To explain the experimental data then, $[QD^*]$ could be several orders of magnitude larger than $[QD]_0$, so that $[QD^*]$ is not greatly changed after charge is transferred to M^+ . For example, if we let $\log(\gamma) = 2$ under illumination, $[QD^*]$ near the working electrode increases to $[QD^*] \approx 10^4 \times [QD]_0$. $[QD^*]$ at the electrode might be higher than $[QD]_0$ if the QDs adsorb to the working electrode or if many electrons accumulate as reduced surface Cd^0 . If we set $[QD^*] = 10^4 \times [QD]_0 = 0.11 \text{ M}$, the experimental CVs with different scan rates can be modeled with only the two reactions corresponding to those in the E_rC_i' mechanism. (**Figure 4**). In this method, the modeled intrinsic rate constants k_{PCT} are on the order of $1 \text{ M}^{-1}\text{s}^{-1}$ and multiplying by $[QD^*]$ again gives observed rates on the order of 0.1 s^{-1} . These observed rates are comparable to those quantified by the direct mathematical calculation from the plateau and peak currents (**Figure 3b**). The two methods of modeling the data give nearly the same simulated CVs in addition to well-matching the experiment (**Figure 4**). We are pleased to report that electrochemical modeling was an effective method of determination of the observed rate because it adds generality to our method. In these experiments, only zones D, KD, and KS were observed, but in other systems reaching these zones may be experimentally constrained, precluding the use of the direct mathematical determination of the rate.

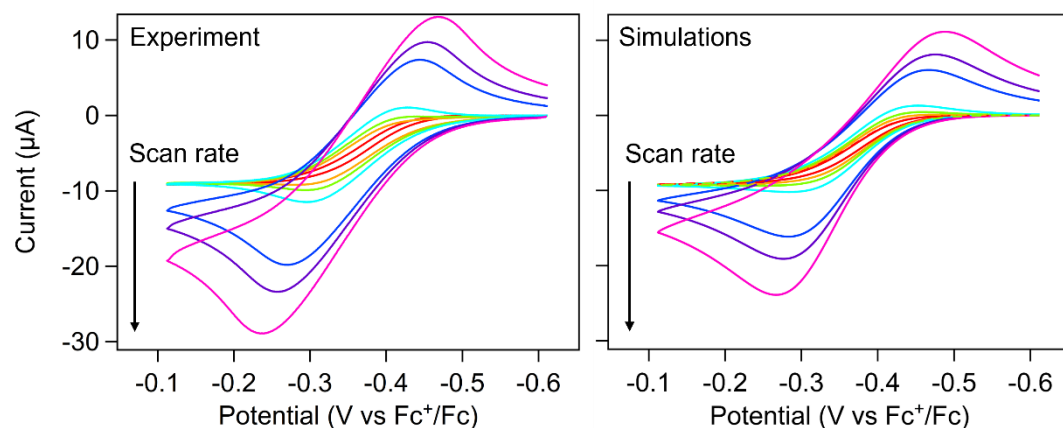


Figure 4. Comparison of the experimental data (left) to the simulated data (right) with the redox probe FcNH₂ with varying scan rate. In the right panel, the simulations with [QD*] = 10⁴ × [QD]₀ are plotted in dashed lines and the simulations with [QD*] = [QD]₀ and regeneration of QD* are plotted in solid lines; these nearly perfectly overlay. 0.1M [TBA][B(C₆F₅)₄], benzonitrile, glassy carbon working, Pt counter, Ag wire pseudo reference electrodes, scan rate was varied from 5 mV/s (red) to 250 mV/s (fuchsia).

Discussion of Photoinduced Charge Transfer to Co(Cp)(dppe), FcNH₂, Fc, FcCOOH, FcCOCH₃

Using both mathematical determination of charge transfer as well as electrochemical modeling, k_{obs} was determined for the range of electron accepting probes. When comparing the mathematical determination and the modeling results (**Figure 3**), k_{obs} was generally comparable. Unsurprisingly, with larger driving force, k_{obs} monotonically increases in both methods of determination. This observation is well supported by existing QD literature, wherein the Marcus inverted region is never observed and photoinduced charge transfer from quantum dots is better explained by other rationalizations.^{9,11,46,47} While others have demonstrated a similar relationship between driving force and rate of charge transfer,^{9,11,48,49} we were uniquely able to measure this through CV.

We have demonstrated that the driving force for photoinduced charge transfer is the critical factor controlling k_{obs} rather than chemical identity. FcCOOH and FcCOCH₃ have nearly the same E^0 but have different chemical interactions with solvent, electrolyte, and the QD ligand shell. Despite these differences, the k_{obs} values for these two redox probes are nearly identical. Therefore, the differences between these redox probes are due to different rates of the pseudo-unimolecular photoinduced charge transfer elementary step (which is directly controlled by the driving force) rather than chemical interactions with the QD. This observation contrasts with studies where the charge acceptor was bound to the quantum dot through a head group, and the identity of this head group controlled the rate of photoinduced charge transfer by controlling the binding equilibrium to the QD surface.¹⁵

The estimated k_{PCT} values are on the order of 1M⁻¹s⁻¹ for the model with high [QD*] and without regeneration and are on the order of 10⁴ M⁻¹s⁻¹ for the model with low [QD*] and regeneration. As a benchmark, the diffusion-controlled rate constant (k_{diff} , the rate assuming every collision results in a charge transferred) is estimated by the Smoluchowski equation (**Eq. 4**), where R_{QD} and R_{M} are the radii of the QD and molecular charge acceptor, respectively, and D_{QD} and D_{M} are the diffusion coefficients (see SI for details).⁵⁰ Importantly, k_{diff} can be directly compared to the result from this work, as both describe bimolecular processes with the same units. Then, $k_{\text{diff}} \sim 10^{10}$ M⁻¹s⁻¹ is at least six orders of magnitude larger than k_{PCT} determined in this work. This implies that productive photoinduced charge transfer is a rare event in these experiments: for one million collisions, less than one charge is effectively transferred to the charge acceptor. We believe the low k_{PCT} helps explain common observations that photocatalytic reactions suffer from extremely poor quantum yield.¹⁸ We attribute the small k_{PCT} to the extremely weak electronic coupling between the inorganic QD core and M in solution. Either charges must tunnel through the ligand shell to reach M in solution or M must bury itself in the ligand shell to get better electronic overlap.⁵¹

$$k_{\text{diff}} = \frac{4\pi N}{1000} (R_{\text{QD}} + R_{\text{M}}) (D_{\text{QD}} + D_{\text{M}}) = 2 \times 10^{10} (\text{M s})^{-1} \quad \text{Eq. 4}$$

Further, we can compare the observed rate constant (k_{obs}) to reported turn over frequencies (TOF) for homogeneous catalysts.²³ In this context, k_{obs} describes the moles of electrons transferred from QD to redox probe, per unit time per mole of the oxidized redox probe in the diffusion layer. Then, the

maximum TOF for the electron acceptors in this work is just the observed rate and is on the order of 0.1 s^{-1} . In comparison, the well-known nitrogenase enzyme, which reduces N_2 to NH_3 , was measured electrochemically to have an electron transfer TOF of 14 s^{-1} .⁵² Similarly, we can compare to photocatalytic systems. In an iridium photocatalytic system tuned for CO_2 reduction, the highest observed TOF was 0.006 s^{-1} .⁵³ In a CdSe QD photocatalytic system tuned for C-O bond cleavage, the TOF was 1.7 s^{-1} .¹⁷ These benchmarks place observed photoinduced electron transfer from QDs faster than reductive photocatalysis in a molecular system, slower than an enzymatic reduction, and about on par with a QD photocatalysis system.

Net hole transfer to CoCp_2

To expand the utility of this method, we considered a probe with lower E^0 : cobaltocenium (CoCp_2^+). In illuminated CV experiments with this redox probe, the oxidative current decreases and the reductive current increases in a manner consistent with the $E_r C_i$ ' mechanism, indicating that there is effective photoinduced hole extraction from the QD to the probe (**Figure 5**). We are particularly excited by this result because it demonstrates that our method for measuring charge transfer can be generalized to hole transfer as well as electron transfer. This is in contrast with spectroscopic characterization, where electron and hole dynamics are difficult to isolate.⁵⁴

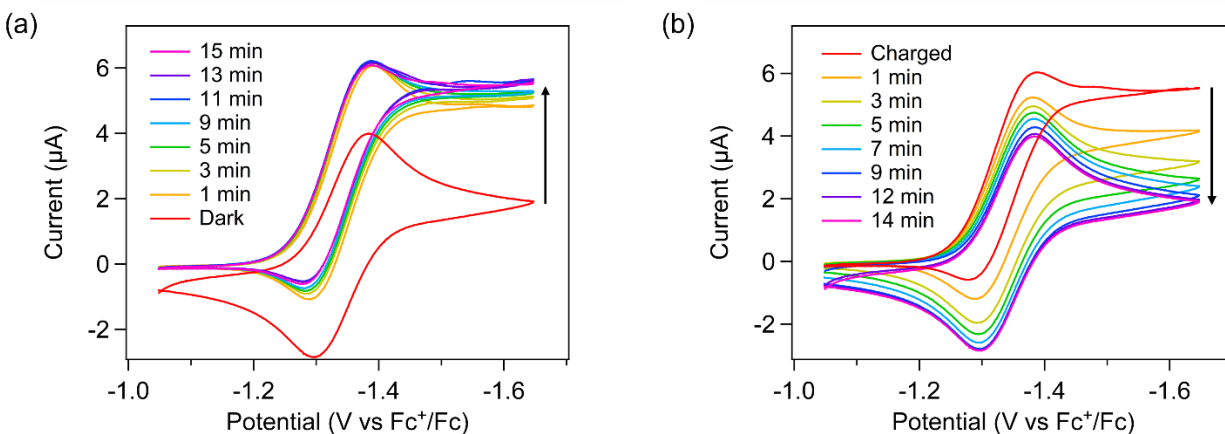


Figure 5. (a) CVs of CoCp_2^+ taken after illumination is begun. (b) CVs of CoCp_2^+ monitored after illumination ends, demonstrating slow depletion of hole donor states. 0.1M $[\text{TBA}][\text{PF}_6]$, benzonitrile, glassy carbon working, Pt counter, Ag wire pseudo reference electrodes, 10 mV/s.

In the CoCp_2^+ solution with QDs, after illumination is begun the CV distorts over several minutes as described above, then the CVs stop changing (**Figure 5a**). Similarly, when illumination is stopped, the CVs take several minutes before overlaying with the trace before illumination (**Figure 5b**). This indicates that, as in the case of electron transfer, the hole-donating species forms over several minutes under illumination before equilibration, and some of these hole-donating species are long-lived. We propose that this long-lived hole-donating species is the hole trap that is populated during the n-type photodoping process and that is slowly depopulated when a conduction band electron recombines with localized holes. Trap mediated hole transfer to molecules has previously been demonstrated in similar QD systems.^{11,48}

In the same manner as the electron acceptor series, the rate of photoinduced hole transfer to CoCp₂ was determined mathematically and through electrochemical modeling. Both methods require knowledge of the concentration of hole-donors, which we estimate is equal to the concentration of the QDs. The mathematical method gives k_{PCT} of $1.38 \times 10^4 \text{ M}^{-1}\text{s}^{-1}$ and the modeling method with $[\text{QD}^*] = 0.11\text{M}$ gives $1.17 \times 10^4 \text{ M}^{-1}\text{s}^{-1}$. Both results are slower than the slowest k_{PCT} in the electron transfer series. This is in good agreement with prior observations that in reductive photocatalysis, hole quenching rather than electron transfer to cocatalyst is rate limiting.^{20,55} Uniquely, we are able to easily disentangle hole transfer dynamics from electron transfer by directly monitoring either oxidation or reduction of the molecular probe.

Conclusion

In this work, cyclic voltammetry has been used for the first time to quantify the rate of photoinduced charge transfer in solution. By carefully designing the photoelectrochemical cell and solvent/electrolyte combination, we were able to simultaneously irradiate and take CV data, generating dynamics that could be readily described by a two-reaction E_rC_i^* mechanism. This technique is a powerful tool for screening photocatalytic systems by directly measuring the effective rate of charge extraction from a photosensitizer. By varying the redox potential of molecular charge acceptors, both net electron and hole transfer from photodoped colloidal quantum dots were observed. Using this technique, we were able to reproduce spectroscopic observation that the rate of photoinduced electron transfer from QDs increases monotonically with driving force. This method is especially compelling because it directly probes the changing oxidation state of the charge acceptor, in contrast with many other techniques that focus on the photophysics of the photosensitizer. The resulting observed rates of charge transfer, on the order of 0.1s^{-1} , are distinct from the spectroscopically measured picosecond dynamics, and report on the rate of generation of charge separated states relevant to photocatalysis.

Supporting Information

Electronic supplementary information (ESI) available: Additional experimental (synthesis and electrochemistry) details, calculations, and supplementary data. See DOI: XXXXXX.

This article is available as a preprint: Homer, M.; Kuo, D.-Y.; Dou, F.; Cossairt, B.*. Photoinduced charge transfer from quantum dots measured by cyclic voltammetry. ChemRxiv, 2022, <https://chemrxiv.org/engage/chemrxiv/article-details/627ac0d959f0d69cf88c0b96>.

Corresponding Author

*cossairt@uw.edu

Funding Sources

National Science Foundation DMR-1719797

Acknowledgements

This material is based upon work supported by the National Science Foundation under award number DMR-1719797. This material is based in part upon work supported by the state of Washington through the University of Washington Clean Energy Institute. Part of this work was conducted at the Molecular Analysis Facility, a National Nanotechnology Coordinated Infrastructure site at the University of Washington which is supported in part by the National Science Foundation (grant NNCI-1542101), the University of Washington, the Molecular Engineering & Sciences Institute, and the Clean Energy Institute.

References

- (1) Qiu, F.; Han, Z.; Peterson, J. J.; Odoi, M. Y.; Sowers, K. L.; Krauss, T. D. Photocatalytic Hydrogen Generation by CdSe/CdS Nanoparticles. *Nano Lett.* **2016**, *16* (9), 5347–5352. <https://doi.org/10.1021/acs.nanolett.6b01087>.
- (2) Yu, W. W.; Qu, L.; Guo, W.; Peng, X. Experimental Determination of the Extinction Coefficient of CdTe, CdSe, and CdS Nanocrystals. *Chem. Mater.* **2003**, *15* (14), 2854–2860. <https://doi.org/10.1021/cm034081k>.
- (3) Rabouw, F. T.; de Mello Donega, C. Excited-State Dynamics in Colloidal Semiconductor Nanocrystals. *Top. Curr. Chem.* **2016**, *374* (5), 58. <https://doi.org/10.1007/s41061-016-0060-0>.
- (4) Graetzel, M.; Frank, A. J. Interfacial Electron-Transfer Reactions in Colloidal Semiconductor Dispersions. Kinetic Analysis. *J. Phys. Chem.* **1982**, *86* (15), 2964–2967. <https://doi.org/10.1021/j100212a031>.
- (5) Wang, X.; Li, C. Interfacial Charge Transfer in Semiconductor-Molecular Photocatalyst Systems for Proton Reduction. *J. Photochem. Photobiol. C Photochem. Rev.* **2017**, *33*, 165–179. <https://doi.org/10.1016/j.jphotochemrev.2017.10.003>.
- (6) Cho, E.; Kim, T.; Choi, S.; Jang, H.; Min, K.; Jang, E. Optical Characteristics of the Surface Defects in InP Colloidal Quantum Dots for Highly Efficient Light-Emitting Applications. *ACS Appl. Nano Mater.* **2018**, *1* (12), 7106–7114. <https://doi.org/10.1021/acsanm.8b01947>.
- (7) Guyot-Sionnest, P.; Shim, M.; Matranga, C.; Hines, M. Intraband Relaxation in CdSe Quantum Dots. *Phys. Rev. B* **1999**, *60* (4), R2181–R2184. <https://doi.org/10.1103/PhysRevB.60.R2181>.
- (8) Morris-Cohen, A. J.; Peterson, M. D.; Frederick, M. T.; Kamm, J. M.; Weiss, E. A. Evidence for a Through-Space Pathway for Electron Transfer from Quantum Dots to Carboxylate-Functionalized Viologens. *J. Phys. Chem. Lett.* **2012**, *3* (19), 2840–2844. <https://doi.org/10.1021/jz301318m>.
- (9) Zhu, H.; Yang, Y.; Wu, K.; Lian, T. Charge Transfer Dynamics from Photoexcited Semiconductor Quantum Dots. *Annu. Rev. Phys. Chem.* **2016**, *67* (1), 259–281. <https://doi.org/10.1146/annurev-physchem-040215-112128>.
- (10) Song, N.; Zhu, H.; Jin, S.; Zhan, W.; Lian, T. Poisson-Distributed Electron-Transfer Dynamics from Single Quantum Dots to C60 Molecules. *ACS Nano* **2011**, *5* (1), 613–621. <https://doi.org/10.1021/nn1028828>.

- (11) Olshansky, J. H.; Balan, A. D.; Ding, T. X.; Fu, X.; Lee, Y. V.; Alivisatos, A. P. Temperature-Dependent Hole Transfer from Photoexcited Quantum Dots to Molecular Species: Evidence for Trap-Mediated Transfer. *ACS Nano* **2017**, *11* (8), 8346–8355. <https://doi.org/10.1021/acsnano.7b03580>.
- (12) Buckley, J. J.; Couderc, E.; Greaney, M. J.; Munteanu, J.; Riche, C. T.; Bradforth, S. E.; Brutchey, R. L. Chalcogenol Ligand Toolbox for CdSe Nanocrystals and Their Influence on Exciton Relaxation Pathways. *ACS Nano* **2014**, *8* (3), 2512–2521. <https://doi.org/10.1021/nn406109v>.
- (13) Morris-Cohen, A. J.; Frederick, M. T.; Cass, L. C.; Weiss, E. A. Simultaneous Determination of the Adsorption Constant and the Photoinduced Electron Transfer Rate for a Cds Quantum Dot–Viologen Complex. *J. Am. Chem. Soc.* **2011**, *133* (26), 10146–10154. <https://doi.org/10.1021/ja2010237>.
- (14) Rawalekar, S.; Kaniyankandy, S.; Verma, S.; Ghosh, H. N. Ultrafast Charge Carrier Relaxation and Charge Transfer Dynamics of CdTe/CdS Core–Shell Quantum Dots as Studied by Femtosecond Transient Absorption Spectroscopy. *J. Phys. Chem. C* **2010**, *114* (3), 1460–1466. <https://doi.org/10.1021/jp909118c>.
- (15) Morris-Cohen, A. J.; Aruda, K. O.; Rasmussen, A. M.; Canzi, G.; Seideman, T.; Kubiak, C. P.; Weiss, E. A. Controlling the Rate of Electron Transfer between a Quantum Dot and a Tri-Ruthenium Molecular Cluster by Tuning the Chemistry of the Interface. *Phys. Chem. Chem. Phys.* **2012**, *14* (40), 13794–13801. <https://doi.org/10.1039/C2CP40827A>.
- (16) Knowles, K. E.; Peterson, M. D.; McPhail, M. R.; Weiss, E. A. Exciton Dissociation within Quantum Dot–Organic Complexes: Mechanisms, Use as a Probe of Interfacial Structure, and Applications. *J. Phys. Chem. C* **2013**, *117* (20), 10229–10243. <https://doi.org/10.1021/jp400699h>.
- (17) Enright, M. J.; Gilbert-Bass, K.; Sarsito, H.; Cossairt, B. M. Photolytic C–O Bond Cleavage with Quantum Dots. *Chem. Mater.* **2019**, *31* (7), 2677–2682. <https://doi.org/10.1021/acs.chemmater.9b00943>.
- (18) Zhang, Z.; Edme, K.; Lian, S.; Weiss, E. A. Enhancing the Rate of Quantum-Dot-Photocatalyzed Carbon–Carbon Coupling by Tuning the Composition of the Dot’s Ligand Shell. *J. Am. Chem. Soc.* **2017**, *139* (12), 4246–4249. <https://doi.org/10.1021/jacs.6b13220>.
- (19) Lu, H.; Zhu, X.; Miller, C.; San Martin, J.; Chen, X.; Miller, E. M.; Yan, Y.; Beard, M. C. Enhanced Photoredox Activity of CsPbBr₃ Nanocrystals by Quantitative Colloidal Ligand Exchange. *J. Chem. Phys.* **2019**, *151* (20), 204305. <https://doi.org/10.1063/1.5129261>.
- (20) Wu, K.; Chen, Z.; Lv, H.; Zhu, H.; Hill, C. L.; Lian, T. Hole Removal Rate Limits Photodriven H₂ Generation Efficiency in CdS–Pt and CdSe/CdS–Pt Semiconductor Nanorod–Metal Tip Heterostructures. *J. Am. Chem. Soc.* **2014**, *136* (21), 7708–7716. <https://doi.org/10.1021/ja5023893>.
- (21) Lian, S.; Weinberg, D. J.; Harris, R. D.; Kodaimati, M. S.; Weiss, E. A. Subpicosecond Photoinduced Hole Transfer from a CdS Quantum Dot to a Molecular Acceptor Bound Through an Exciton-Delocalizing Ligand. *ACS Nano* **2016**, *10* (6), 6372–6382. <https://doi.org/10.1021/acsnano.6b02814>.
- (22) Woodward, J. R. Radical Pairs in Solution. *Prog. React. Kinet. Mech.* **2002**, *27* (3), 165–207. <https://doi.org/10.3184/007967402103165388>.
- (23) Rountree, E. S.; McCarthy, B. D.; Eisenhart, T. T.; Dempsey, J. L. Evaluation of Homogeneous Electrocatalysts by Cyclic Voltammetry. *Inorg. Chem.* **2014**, *53* (19), 9983–10002. <https://doi.org/10.1021/ic500658x>.

- (24) Costentin, C.; Fortage, J.; Collomb, M.-N. Electrophotocatalysis: Cyclic Voltammetry as an Analytical Tool. *J. Phys. Chem. Lett.* **2020**, *11* (15), 6097–6104. <https://doi.org/10.1021/acs.jpcclett.0c01662>.
- (25) Fukatsu, A.; Kondo, M.; Okamura, M.; Yoshida, M.; Masaoka, S. Electrochemical Response of Metal Complexes in Homogeneous Solution under Photoirradiation. *Sci. Rep.* **2014**, *4* (1), 5327. <https://doi.org/10.1038/srep05327>.
- (26) Henckel, D. A.; Enright, M. J.; Panahpour Eslami, N.; Kroupa, D. M.; Gamelin, D. R.; Cossairt, B. M. Modeling Equilibrium Binding at Quantum Dot Surfaces Using Cyclic Voltammetry. *Nano Lett.* **2020**, *20* (4), 2620–2624. <https://doi.org/10.1021/acs.nanolett.0c00162>.
- (27) Fox, M. A.; Akaba, R. Curve Crossing in the Cyclic Voltammetric Oxidation of 2-Phenylnorbornene. Evidence for an ECE Reaction Pathway. *J. Am. Chem. Soc.* **1983**, *105* (11), 3460–3463. <https://doi.org/10.1021/ja00349a014>.
- (28) Araujo, J. J.; Brozek, C. K.; Kroupa, D. M.; Gamelin, D. R. Degenerately N-Doped Colloidal PbSe Quantum Dots: Band Assignments and Electrostatic Effects. *Nano Lett.* **2018**, *18* (6), 3893–3900. <https://doi.org/10.1021/acs.nanolett.8b01235>.
- (29) Wu Lizhu; Huan Maoyong; Li Xubing; Zhou Shuai; Zhang Liping; Tong Zhenhe. Method for Photocatalytic Halogenation Conversion of Halogenated Hydrocarbon Using Quantum Dot/Rod Photocatalyst. CN109438156A, March 8, 2019.
- (30) De Roo, J.; Yazdani, N.; Drijvers, E.; Lauria, A.; Maes, J.; Owen, J. S.; Van Driessche, I.; Niederberger, M.; Wood, V.; Martins, J. C.; Infante, I.; Hens, Z. Probing Solvent–Ligand Interactions in Colloidal Nanocrystals by the NMR Line Broadening. *Chem. Mater.* **2018**, *30* (15), 5485–5492. <https://doi.org/10.1021/acs.chemmater.8b02523>.
- (31) Monahan, M.; Homer, M.; Zhang, S.; Zheng, R.; Chen, C.-L.; De Yoreo, J.; Cossairt, B. M. Impact of Nanoparticle Size and Surface Chemistry on Peptoid Self-Assembly. *ACS Nano* **2022**. <https://doi.org/10.1021/acsnano.2c01203>.
- (32) Geiger, W. E.; Barrière, F. Organometallic Electrochemistry Based on Electrolytes Containing Weakly-Coordinating Fluoroarylborate Anions. *Acc. Chem. Res.* **2010**, *43* (7), 1030–1039. <https://doi.org/10.1021/ar1000023>.
- (33) Swarts, P. J.; Conradie, J. Solvent and Substituent Effect on Electrochemistry of Ferrocenylcarboxylic Acids. *J. Electroanal. Chem.* **2020**, *866*, 114164. <https://doi.org/10.1016/j.jelechem.2020.114164>.
- (34) Shulenberg, K. E.; Keller, H. R.; Pellows, L. M.; Brown, N. L.; Dukovic, G. Photocharging of Colloidal CdS Nanocrystals. *J. Phys. Chem. C* **2021**, *125* (41), 22650–22659. <https://doi.org/10.1021/acs.jpcc.1c06491>.
- (35) Zeng, Y.; Kelley, D. F. Excited Hole Photochemistry of CdSe/CdS Quantum Dots. *J. Phys. Chem. C* **2016**, *120* (31), 17853–17862. <https://doi.org/10.1021/acs.jpcc.6b06282>.
- (36) Tsui, E. Y.; Carroll, G. M.; Miller, B.; Marchioro, A.; Gamelin, D. R. Extremely Slow Spontaneous Electron Trapping in Photodoped N-Type CdSe Nanocrystals. *Chem. Mater.* **2017**, *29* (8), 3754–3762. <https://doi.org/10.1021/acs.chemmater.7b00839>.

- (37) Hartley, C. L.; Dempsey, J. L. Electron-Promoted X-Type Ligand Displacement at CdSe Quantum Dot Surfaces. *Nano Lett.* **2019**, *19* (2), 1151–1157. <https://doi.org/10.1021/acs.nanolett.8b04544>.
- (38) du Fossé, I.; ten Brinck, S.; Infante, I.; Houtepen, A. J. Role of Surface Reduction in the Formation of Traps in N-Doped II–VI Semiconductor Nanocrystals: How to Charge without Reducing the Surface. *Chem. Mater.* **2019**, *31* (12), 4575–4583. <https://doi.org/10.1021/acs.chemmater.9b01395>.
- (39) Giansante, C.; Infante, I. Surface Traps in Colloidal Quantum Dots: A Combined Experimental and Theoretical Perspective. *J. Phys. Chem. Lett.* **2017**, *8* (20), 5209–5215. <https://doi.org/10.1021/acs.jpcclett.7b02193>.
- (40) Zhao, J.; Holmes, M. A.; Osterloh, F. E. Quantum Confinement Controls Photocatalysis: A Free Energy Analysis for Photocatalytic Proton Reduction at CdSe Nanocrystals. *ACS Nano* **2013**, *7* (5), 4316–4325. <https://doi.org/10.1021/nn400826h>.
- (41) Deblock, L.; Goossens, E.; Pokratath, R.; De Buysser, K.; De Roo, J. Mapping out the Aqueous Surface Chemistry of Metal Oxide Nanocrystals: Carboxylate, Phosphonate, and Catecholate Ligands. *JACS Au* **2022**, *2* (3), 711–722. <https://doi.org/10.1021/jacsau.1c00565>.
- (42) Kanicky, J. R.; Shah, D. O. Effect of Degree, Type, and Position of Unsaturation on the PKa of Long-Chain Fatty Acids. *J. Colloid Interface Sci.* **2002**, *256* (1), 201–207. <https://doi.org/10.1006/jcis.2001.8009>.
- (43) Cohn, A. W.; Rinehart, J. D.; Schimpf, A. M.; Weaver, A. L.; Gamelin, D. R. Size Dependence of Negative Trion Auger Recombination in Photodoped CdSe Nanocrystals. *Nano Lett.* **2014**, *14* (1), 353–358. <https://doi.org/10.1021/nl4041675>.
- (44) Tsui, E. Y.; Hartstein, K. H.; Gamelin, D. R. Selenium Redox Reactivity on Colloidal CdSe Quantum Dot Surfaces. *J. Am. Chem. Soc.* **2016**, *138* (35), 11105–11108. <https://doi.org/10.1021/jacs.6b06548>.
- (45) Hughes, K. E.; Hartstein, K. H.; Gamelin, D. R. Photodoping and Transient Spectroscopies of Copper-Doped CdSe/CdS Nanocrystals. *ACS Nano* **2018**, *12* (1), 718–728. <https://doi.org/10.1021/acsnano.7b07879>.
- (46) Wang, L.-W.; Califano, M.; Zunger, A.; Franceschetti, A. Pseudopotential Theory of Auger Processes in CdSe Quantum Dots. *Phys. Rev. Lett.* **2003**, *91* (5), 056404. <https://doi.org/10.1103/PhysRevLett.91.056404>.
- (47) Harvie, A. J.; Smith, C. T.; Ahumada-Lazo, R.; Jeuken, L. J. C.; Califano, M.; Bon, R. S.; Hardman, S. J. O.; Binks, D. J.; Critchley, K. Ultrafast Trap State-Mediated Electron Transfer for Quantum Dot Redox Sensing. *J. Phys. Chem. C* **2018**, *122* (18), 10173–10180. <https://doi.org/10.1021/acs.jpcc.8b02551>.
- (48) Olshansky, J. H.; Ding, T. X.; Lee, Y. V.; Leone, S. R.; Alivisatos, A. P. Hole Transfer from Photoexcited Quantum Dots: The Relationship between Driving Force and Rate. *J. Am. Chem. Soc.* **2015**, *137* (49), 15567–15575. <https://doi.org/10.1021/jacs.5b10856>.
- (49) Nagelj, N.; Brumberg, A.; Peifer, S.; Schaller, R. D.; Olshansky, J. H. Compositionally Tuning Electron Transfer from Photoexcited Core/Shell Quantum Dots via Cation Exchange. *J. Phys. Chem. Lett.* **2022**, 3209–3216. <https://doi.org/10.1021/acs.jpcclett.2c00333>.

- (50) Joseph Lakowicz. *Principles of Fluorescence Spectroscopy*, 3rd ed.; Springer: Baltimore, 2006.
- (51) Huang, Y.; Cohen, T. A.; Sperry, B. M.; Larson, H.; Nguyen, H. A.; Homer, M. K.; Dou, F. Y.; Jacoby, L. M.; Cossairt, B. M.; Gamelin, D. R.; Luscombe, C. K. Organic Building Blocks at Inorganic Nanomaterial Interfaces. *Mater. Horiz.* **2022**, *9* (1), 61–87. <https://doi.org/10.1039/D1MH01294K>.
- (52) Gu, W.; Milton, R. D. Natural and Engineered Electron Transfer of Nitrogenase. *Chemistry* **2020**, *2* (2), 322–346. <https://doi.org/10.3390/chemistry2020021>.
- (53) Genoni, A.; Chirdon, D. N.; Boniolo, M.; Sartorel, A.; Bernhard, S.; Bonchio, M. Tuning Iridium Photocatalysts and Light Irradiation for Enhanced CO₂ Reduction. *ACS Catal.* **2017**, *7* (1), 154–160. <https://doi.org/10.1021/acscatal.6b03227>.
- (54) Morgan, D. P.; Kelley, D. F. What Does the Transient Absorption Spectrum of CdSe Quantum Dots Measure? *J. Phys. Chem. C* **2020**, *124* (15), 8448–8455. <https://doi.org/10.1021/acs.jpcc.0c02566>.
- (55) Berr, M. J.; Wagner, P.; Fischbach, S.; Vaneski, A.; Schneider, J.; Susha, A. S.; Rogach, A. L.; Jäckel, F.; Feldmann, J. Hole Scavenger Redox Potentials Determine Quantum Efficiency and Stability of Pt-Decorated CdS Nanorods for Photocatalytic Hydrogen Generation. *Appl. Phys. Lett.* **2012**, *100* (22), 223903. <https://doi.org/10.1063/1.4723575>.

TOC Graphic

